

Polymer Donors with A New Electron-Deficient Unit for Efficient Organic Solar Cells

Zhe Zhang^{†[a]}, Tianqi Chen^{†[b]}, Xuehang Dong^[b], Haoyu Li^[a], Tainan Duan^[c], Ekaterina A. Knyazeva^[d], Alexandra S. Chechulina^[d], Oleg A. Rakitin^[d], Bin Kan^[b], Xiangjian Wan^[a], Yongsheng Chen^{*[a]}

[a] The Centre of Nanoscale Science and Technology and Key Laboratory of Functional Polymer Materials, Institute of Polymer Chemistry, State Key Laboratory of Elemento-Organic Chemistry, Renewable Energy Conversion and Storage Center (RECAST), Frontiers Science Center for New Organic Matter, College of Chemistry, Nankai University, Tianjin 300071, China.

[b] School of Materials Science and Engineering, National Institute for Advanced Materials, Nankai University, Tianjin 300350, China.

[c] Chongqing Institute of Green and Intelligent Technology, Chongqing School, University of Chinese Academy of Sciences, Chinese Academy of Sciences.

[d] N. D. Zelinsky Institute of Organic Chemistry, Russian Academy of Sciences, 47 Leninsky prosp., 119991 Moscow, Russian Federation.

†These authors contributed equally.

Corresponding E-mails: yschen99@nankai.edu.cn (Y.C.)

Contents

1. Materials and Methods

2. Synthesis of PD1 and PD2

3. Supporting Figures (S1-18) and Tables (S1-8)

4. References

1. Materials and Methods

Non-fullerene acceptor L8-BO, (4,8-bis(5-(2-ethylhexyl)-4-fluorothiophen-2-yl)benzo[1,2-b:4,5-b']dithiophene-2,6-diyl)bis(trimethylsilane)—BDT-F, and (4,8-bis(5-(2-ethylhexyl)thiophen-2-yl)benzo[1,2-b:4,5-b']dithiophene-2,6-diyl)bis(trimethylsilane)—BDT were purchased from Solarmer Material (Beijing) Inc, Organtec. Ltd, Woerjiming (Beijing) Technology Development Institute, respectively. Starting material **1** were synthesized according to our previously reported method¹. All chemicals and other reagents, unless otherwise specified, were purchased from commercial suppliers and were directly used without further purification.

Computational methods in this work. The structures were subsequently optimized with Density Functional Theory (DFT) in vacuum within the Gaussian 16 software. The structure optimization, frequency analysis and energy level of frontier molecular orbital were obtained at the Becke three-parameter Lee-Yang-Parr (B3LYP) hybrid functional with the 6-31G(d) basis set.

Molecular weight and polydispersity index measurement. To measure the molecular weight and polydispersity index of polymer donors, gel permeation chromatography (GPC) measurement was carried out on a Waters E2695 instrument using trichlorobenzene (TCB) as eluent at 150 °C.

Thermogravimetric analysis (TGA) and Differential Scanning Calorimetry (DSC). TGA and DSC measurements were performed on a TG209 DSC204 DMA242 METTLER3+ DSC instrument with a heating rate of 10 °C min⁻¹ under a nitrogen atmosphere.

UV-visible (UV-*Vis*) absorption and Variable-temperature UV-*Vis* absorption. UV-vis absorption spectra and Variable-temperature UV-*Vis* absorption spectra were recorded on a Cary 5000 UV-vis spectrophotometer.

Electrochemical characterizations. The cyclic voltammetry (CV) was performed on a LK98B II Microcomputer-based Electrochemical Analyzer using a glassy carbon electrode as the working electrode, a saturated calomel electrode (SCE) as reference electrode, and a Pt wire as the counter electrode. The sample film on working electrode was in an acetonitrile solution of 0.1 mol L⁻¹ n-Bu₄NPF₆ at a scan rate of 100 mV s⁻¹. The ferrocene/ferrocenium was employed as internal reference. The HOMO and LUMO levels were calculated using the following equations: $E_{\text{HOMO}} = -(E_{\text{ox}} + 4.8 - E_{\text{Fc/Fc}^+})$ eV, $E_{\text{LUMO}} = -(E_{\text{red}} + 4.8 - E_{\text{Fc/Fc}^+})$ eV.

Photoluminescent (PL). The steady-state photoluminescence was measured via a

FLS1000 equipment. The emission spectra of PD-1, PD-2 and L8-BO were recorded by NIR 5509 PMT, respectively. The PD-1 and PD-2 was excited at 500 nm. The L8-BO were excited at 760 nm.

EQE_{EL} and FTPS-EQE. The OSCs used for the FTPS-EQE spectra measurements are the same with those of the J - V measurements, with a conventional device structure of ITO/PEDOT:PSS/Active layer/PNDIT-F3N/Ag. EQE_{EL} measurements were performed by applying external voltage/current sources through the devices (REPS, Enlitech). The FTPS-EQE measurement was carried out on an Enlitech FTPS PECT-600 instrument.

Measurements of Transient Photocurrent (TPV). The TPC measurements were performed on a Molex 180081-4320 with a light intensity of about 0.5 sun. Voltage and current dynamics were recorded on a digital oscilloscope (Tektronix MDO4104C), and voltages at open circuit and currents under short circuit conditions were measured over a 50 Ω resistor, respectively.

Atomic force microscopy (AFM). The AFM images were obtained from a Bruker Dimension Icon atomic force microscope by using in tapping mode. The film samples were prepared under the same conditions as those used for device fabrication.

Grazing incidence wide angle X-ray scattering (GIWAXS). The GIWAXS data was obtained at in a Xeuss 3.0 SAXS/WAXS system with a wavelength of $\lambda = 1.341 \text{ \AA}$ at Vacuum Interconnected Nanotech Workstation (Nano-X). The exposure time was 10 minutes. The film samples on the Si substrate were prepared under the same conditions as those used for device fabrication.

Transient photocurrent (TPC). The TPC measurements were performed on a Molex 180081-4320 with a light intensity of about 0.5 sun. Current dynamics were recorded on a digital oscilloscope (Tektronix MDO4104C), and currents under short circuit conditions were measured over a 50 Ω resistor, respectively.

Space-charge-limited current (SCLC) measurement. The SCLC method was used to measure the hole and electron mobilities, by using a diode configuration of ITO/PEDOT:PSS/active layer/MoO₃/Al for hole-only device and ITO/ZnO/active layer/PNDIT-F3N/Al for electron-only device. In our case, we applied forward scans for all the SCLC measurements, and hence the ITO and Al electrodes should be the anode and cathode, respectively. The dark current density curves were recorded with a bias voltage in the range of 0-8 V. The mobilities were estimated by taking current-voltage curves and fitting the results based on the equation listed below:

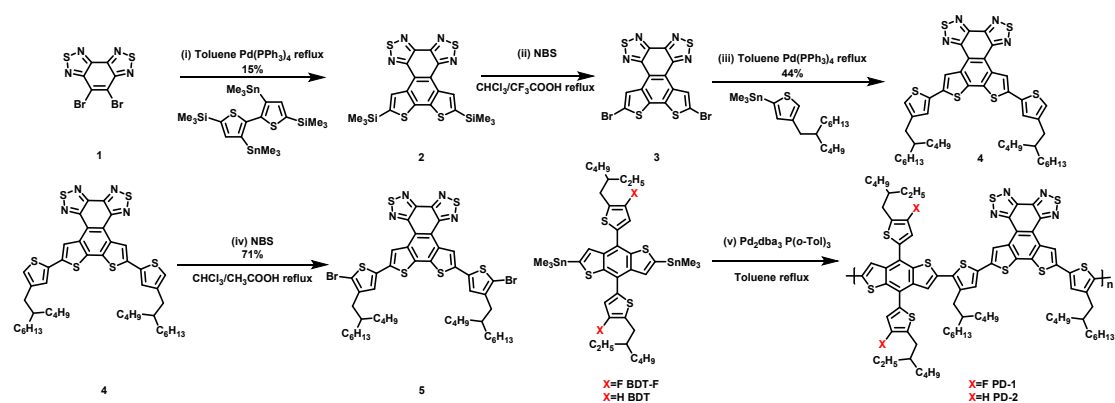
$$J = \frac{9\varepsilon_0\varepsilon_r\mu V^2}{8L^3}$$

where J is the current density, ε_0 is the vacuum permittivity, ε_r is the relative dielectric constant, μ is the mobility, and L is the film thickness. $V (=V_{\text{app}} - V_{\text{bi}})$ is the internal voltage in the device, where V_{app} is the applied voltage to the device and V_{bi} is the built-in voltage due to the relative work function difference of the two electrodes.

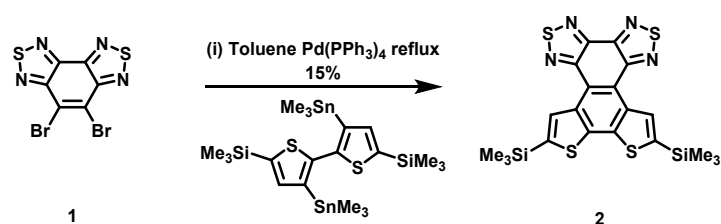
Device fabrication and measurement. The conventional devices were fabricated with an architecture of ITO/PEDOT:PSS (4083)/Polymer donors: L8-BO/PNDIT-F3N/Ag. In detail, the ITO glass was pre-cleaned in turn in an ultrasonic bath of detergent, deionized water, acetone and isopropanol. Then the surface of ITO was treated by UV light in an ultraviolet-ozone chamber (Jelight Company) for 15 min. A thin layer of PEDOT: PSS was deposited on the ITO substrate by spin-coating a PEDOT:PSS solution (Baytron P VP AI 4083) at 4300 rpm for 20 s and then dried at 150 °C for 20 mins in air. Then the substrates were transferred to a glovebox filled with nitrogen. The blends with solid additives were fully dissolved in chloroform (CF) at a concentration of 7 mg/mL (5.5 mg/mL) of PD-1 (PD-2). The resulting solutions were stirred at room temperature for 6 hours and then spin-casted at 2000 rpm for 30 s onto the PEDOT:PSS layer. The PD-1:L8-BO solution (1:1.4 by weight) were stirred at room temperature for 6 hours before coating on the ITO/PEDOT:PSS substrate. The PD-2:L8-BO solution (1:1 by weight) were stirred at room temperature for 6 hours before coating on the ITO/PEDOT:PSS substrate. The films of PD-1:L8-BO were treated with the thermal annealing at 90°C for 6 min. The films of PD-2:L8-BO were treated with the thermal annealing at 100°C for 5 min. The thickness of all active layers was controlled to be ~100 nm. After that, a thin layer of PNDIT-F3N (dissolved in methanol with the concentration of 1 mg/mL) was spin-coated on the top of the active layer. Finally, a layer of Ag with thickness of 150 nm was deposited under 2×10^{-6} Pa. The active area of the device was 0.04 cm². The current density-voltage (J - V) curves of photovoltaic devices were recorded by a Keithley 2400 source-measure unit. The photocurrent was measured under the simulated illumination of 100 mW cm⁻² with AM1.5 G using a Enli SS-F5-3A solar simulator, which was calibrated by a standard Si solar cell (made by Enli Technology Co., Ltd., Taiwan, and calibrated report can be traced to NREL). The thickness of the active layers was measured by a Veeco Dektak 150 profilometer. The EQE spectra were measured by using a QE-R Solar Cell. Response Measurement

System (Enli Technology Co., Ltd., Taiwan).

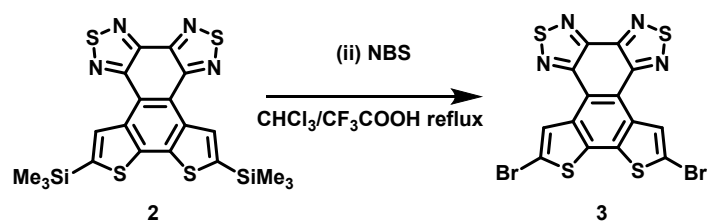
2. Synthesis of PD-1 and PD-2.



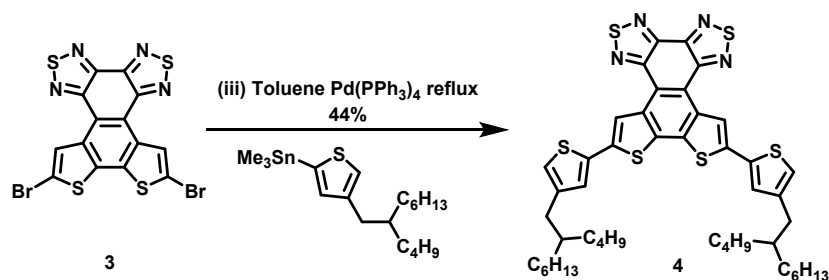
Scheme S1. The synthetic route of PD-1 and PD-2. Reagents and conditions: (i) (3,3'-bis(trimethylstannyl)-[2,2'-bithiophene]-5,5'-diyl)bis(trimethylsilane), Pd(PPh₃)₄, toluene, reflux; (ii) 1-bromopyrrolidine-2,5-dione, CHCl₃/CF₃COOH (2:1), reflux; (iii) (4-(2-butyl-octyl)thiophen-2-yl)trimethylstannane, Pd(PPh₃)₄, toluene, reflux; (iv) 1-bromopyrrolidine-2,5-dione, CHCl₃/CH₃COOH (1:1), reflux; (v) BDT-F or BDT, Pd₂dba₃, P(o-Tol)₃, toluene, reflux.



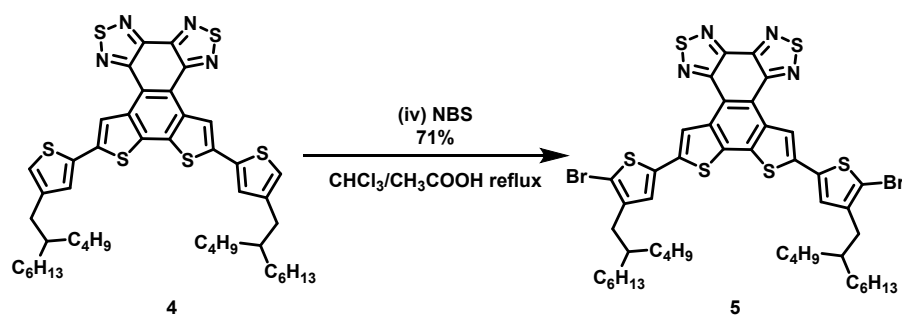
Scheme S2. Synthesis of compound 2. The key compound **1** was synthesized according to previous reports¹. Compound (3,3'-bis(trimethylstannyl)-[2,2'-bithiophene]-5,5'-diyl)bis(trimethylsilane) was synthesized according to previously reported methods². Compound **1** (2 g, 5.68 mmol, 1.0 eq.), (3,3'-bis(trimethylstannyl)-[2,2'-bithiophene]-5,5'-diyl)bis(trimethylsilane) (3.61 g, 5.68 mmol, 1.0 eq.), Pd(PPh₃)₄ (656 mg, 0.568 mmol, 0.1 eq.) and 15 mL toluene was added to 100 mL two-necked round bottom flask. The flask was purged with argon and sealed under argon flow. The resulting mixture was stirred and heated to reflux for 16 h. Then the mixture was allowed to warm to room temperature, and extracted with dichloromethane (3 × 75 mL). The combined organic phase was dried over Na₂SO₄, filtrated, and concentrated under vacuum. The crude product was purified by column chromatography on silica gel with petroleum ether/dichloromethane (v/v = 2/1) as the eluent to give compound **2** as a white solid (414 mg, 15%). ¹H NMR (400 MHz, CDCl₃) δ 9.32 (s, 2H), 0.54 (s, 18H). ¹³C NMR (101 MHz, CDCl₃) δ 156.00, 147.68, 143.13, 140.88, 134.70, 133.69, 119.82. HR-MS (*m/z*, MALDI): Calc. for C₂₀H₂₀N₄S₄Si₂ [M]⁺ 500.8180, found: 500.0103.



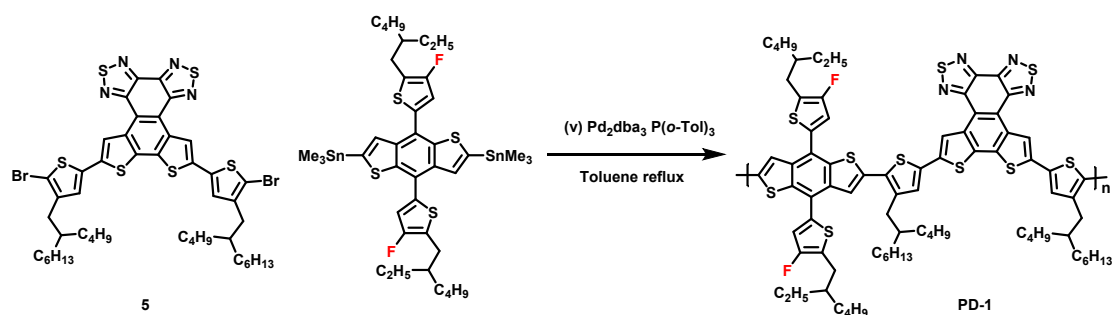
Scheme S2. Synthesis of compound 3. Under the protection of argon, compound **2** (350 mg, 699 μmol , 1.0 eq.), 1-bromopyrrolidine-2,5-dione (274 mg, 1.54 mmol, 2.2 eq.), and 20 mL CHCl_3 was added to 100 mL two-necked round bottom flask. Then 10 mL CF_3COOH was added to the mixture. The mixture was stirred at 80 $^\circ\text{C}$ overnight. After cooling to rt, the mixture was poured into MeOH (200 ml). The precipitate was collected by filtration and dried under vacuum to give compound **5** as an orange solid (284 mg). NMR data of were not acquired due to the extremely low solubility of compound **3**.



Scheme S3. Synthesis of compound 4. Under argon protection, compound **3** (284 mg, 552 μmol , 1.0 eq.), (4-(2-butyl-octyl)thiophen-2-yl)trimethylstannane (688 mg, 1.66 mmol, 3.0 eq.), $\text{Pd}(\text{PPh}_3)_4$ (64 mg, 55 μmol , 0.1 eq.) and toluene (40 mL) was added to 100 mL two-necked round bottom flask. Then the mixture was stirred and heated at 120 $^\circ\text{C}$ overnight. The mixture was allowed to warm to room temperature, and extracted with dichloromethane (3×75 mL). The combined organic phase was dried over Na_2SO_4 , filtrated, and concentrated under vacuum. The crude product was purified by column chromatography on silica gel with petroleum ether/dichloromethane ($v/v = 2/1$) as the eluent to give compound **4** as a yellow solid (207 mg, 44%). ^1H NMR (400 MHz, CDCl_3) δ 8.54 (s, 2H), 7.01 (s, 2H), 6.94 (s, 2H), 2.62 (d, $J = 6.9$ Hz, 4H), 1.76-1.69 (m, 2H), 1.44-1.31 (m, 32H), 1.00-0.91 (m, 12H). HR-MS (m/z , MALDI): Calc. for $\text{C}_{46}\text{H}_{56}\text{N}_4\text{S}_6$ $[\text{M}]^+$ 857.3420, found: 856.2824.

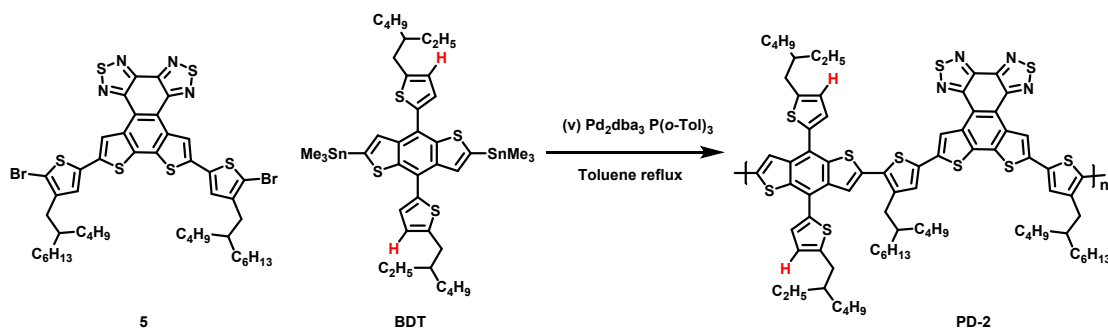


Scheme S4. Synthesis of compound 5. Compound 4 (207 mg, 241 μmol , 1.0 eq.) was added to CHCl_3 (15 mL) and CH_3COOH (15 mL). After the solid dissolved completely, N-bromosuccinimide (NBS) (95 mg, 531 μmol , 2.2 eq.) was added in one portion at 0 $^\circ\text{C}$. Then the mixture was stirred and heated at 80 $^\circ\text{C}$ overnight. The mixture was allowed to warm to room temperature, and extracted with dichloromethane (3×75 mL). The combined organic phase was dried over Na_2SO_4 , filtrated, and concentrated under vacuum. The crude product was purified by column chromatography on silica gel with petroleum ether/dichloromethane ($v/v = 3/2$) as the eluent to give compound **5** as a yellow solid (174 mg, 71%). ^1H NMR (400 MHz, CDCl_3) δ 7.94 (s, 2H), 6.60 (s, 2H), 2.51 (d, $J = 6.9$ Hz, 4H), 1.80-1.72 (m, 2H), 1.44-1.34 (m, 32H), 1.02-0.92 (m, 12H). ^{13}C NMR (101 MHz, CDCl_3) δ 154.21, 146.69, 142.54, 136.61, 135.85, 133.40, 132.81, 126.49, 121.15, 117.89, 110.79, 34.45, 33.62, 33.21, 32.17, 30.02, 28.96, 26.74, 23.39, 22.95, 14.48, 14.40. HR-MS (m/z , MALDI): Calc. for $\text{C}_{46}\text{H}_{54}\text{Br}_2\text{N}_4\text{S}_6$ $[\text{M}]^+$ 1015.1340, found: 1014.1020.



Scheme S5. Synthesis of compound PD-1. Compound 5 (101.51 mg, 0.1 mmol, 1.0 eq.), BDT-F (94.05 mg, 0.1 mmol, 1.0 eq.), $\text{Pd}_2(\text{dba})_3$ (2.75 mg, 3 μmol , 0.03 eq.), $\text{P}(o\text{-Tol})_3$ (9.14 mg, 0.3 mmol, 0.3 eq.) and 5 mL toluene was added to 25 mL two-necked round bottom flask. The flask was purged with argon and sealed under argon flow. The resulting mixture was stirred and heated to reflux for 24 h. After being cooled to room temperature, the mixture was poured into methanol (50 mL) and filtered. The polymer was subjected to Soxhlet extractions with methanol, dichloromethane, and chloroform each for 12 hours, respectively. The chloroform solution was concentrated and

precipitated in methanol to afford PD-1 as a red solid (127 mg 65%). GPC: Mn=19.1 kDa, Mw=53.1 kDa, PDI= 2.77.



Scheme S5. Synthesis of compound PD-2. Compound 5 (101.51 mg, 0.1 mmol, 1.0 eq.), BDT (90.46 mg, 0.1 mmol, 1.0 eq.), Pd₂(dba)₃ (2.75 mg, 3 μmol, 0.03 eq.), P(*o*-tol)₃ (9.14 mg, 0.3 mmol, 0.3 eq.) and 5 mL toluene was added to 25 mL two-necked round bottom flask. The flask was purged with argon and sealed under argon flow. The resulting mixture was stirred and heated to reflux for 24 h. After being cooled to room temperature, the mixture was poured into methanol (50 mL) and filtered. The polymer was subjected to Soxhlet extractions with methanol, dichloromethane, and chloroform each for 12 hours, respectively. The chloroform solution was concentrated and precipitated in methanol to afford PD-2 as a red solid (127 mg 65%). GPC: Mn=47.7 kDa, Mw=95.6 kDa, PDI= 2.18.

3. Figures and tables

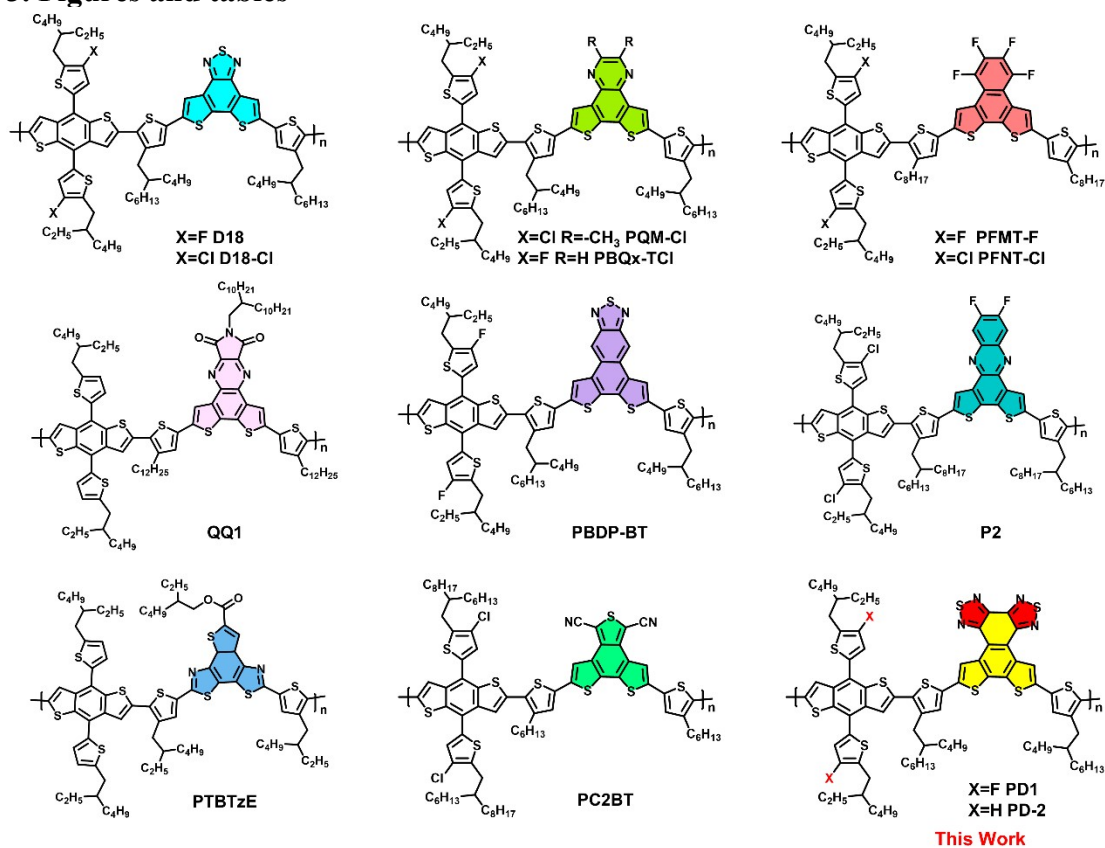


Figure S1. Efficient polymer donors with different large fused electron-deficient units.

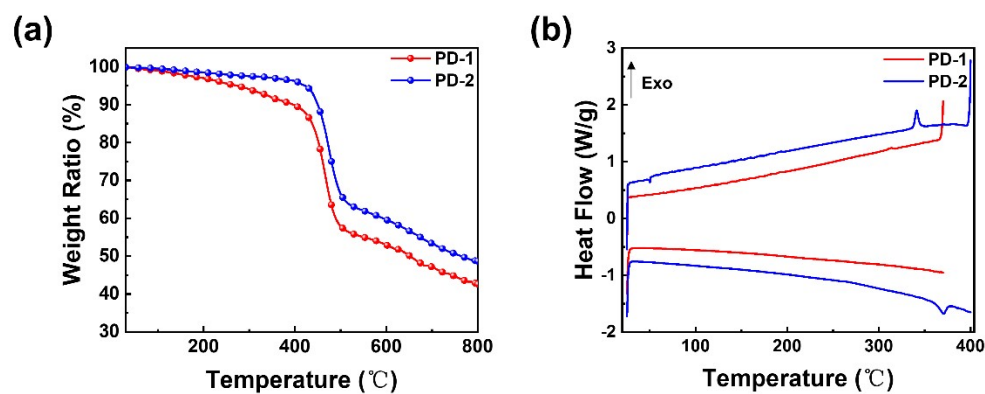


Figure S2. (a) Thermogravimetric analysis (TGA) curves of PD-1 and PD-2; (2) Differential scanning calorimetry (DSC) curves of PD-1 and PD-2.

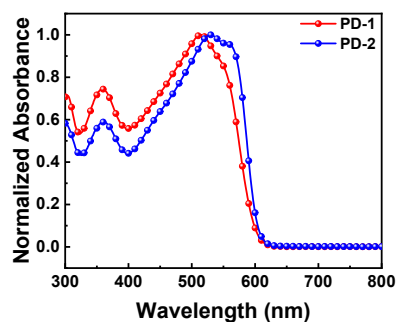


Figure S3. UV-vis absorption spectra of PD-1 and PD-2 in chloroform solutions.

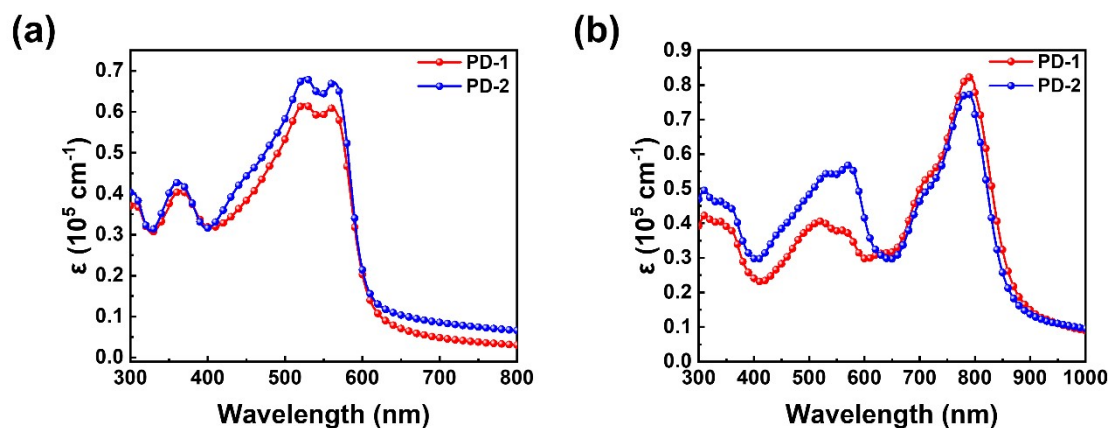


Figure S4. The extinction coefficients of PD-1 and PD-2 in (a) pristine and (b) blend films.

Table S1. Summary of physicochemical data of PD-1 and PD-2.

Comp.	$\lambda_{\max}^{\text{sol}}$ (nm)	$\lambda_{\max}^{\text{film}}$ (nm)	$\lambda_{\text{edge}}^{\text{film}}$ (nm)	$E_{\text{g onset}}$ (eV)	HOMO (eV)	LUMO (eV)
PD-1	513	522	609	2.04	-5.64	-2.77
PD-2	528	565	613	2.02	-5.63	-2.75

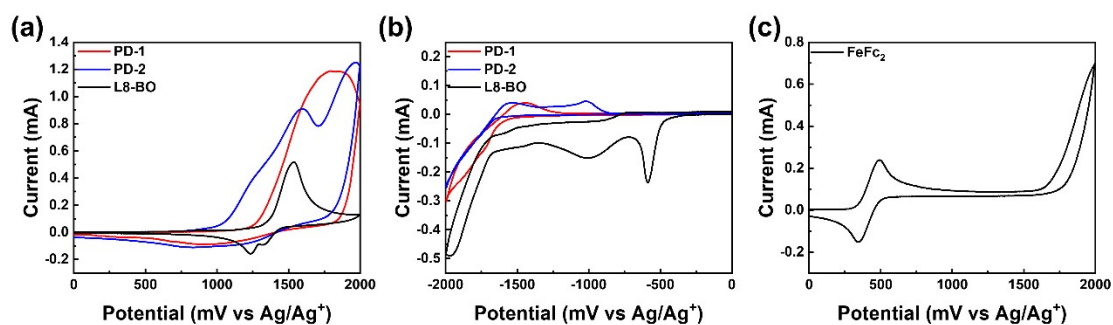


Figure S4. (a) Cyclic voltammograms of the oxidation of PD-1, PD-2 and L8-BO films; (b) Cyclic voltammograms of the reduction of PD-1, PD-2 and L8-BO films; (c) Cyclic voltammogram of ferrocene.

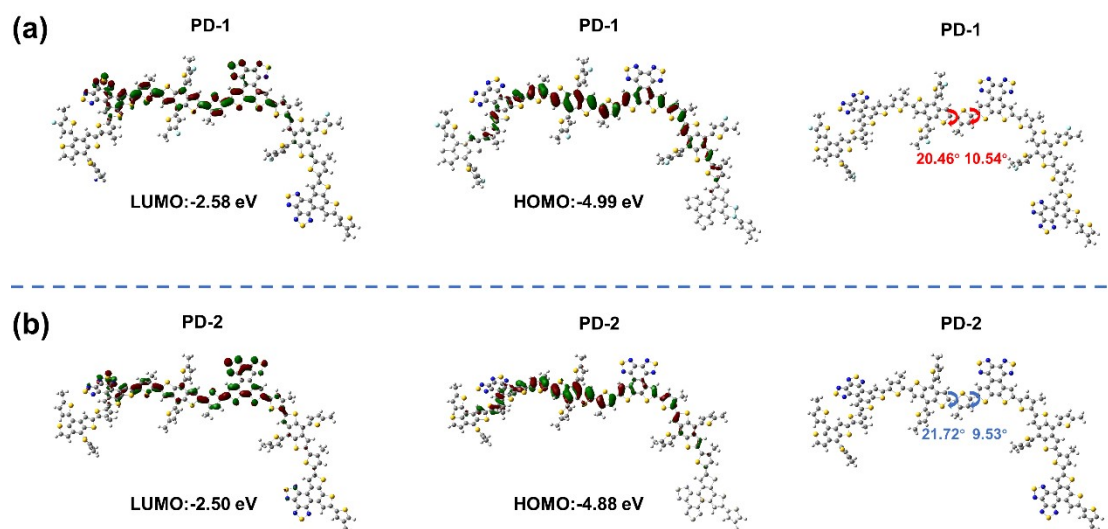


Figure S5. The calculated frontier molecular orbits and optimized trimers structures of (a) PD-1 and (b) PD-2 in front view.

Table S2. Photovoltaic performance of the solar cells based on **PD-1:L8-BO** with different D:A ratios under the illumination of AM 1.5G.

D:A	TA	V_{oc} (V)	J_{sc} (mA·cm ⁻²)	FF (%)	PCE (%)
1:0.8	90°C/6 mins	0.977	8.49	29.4	2.44
1:1	90°C/6 mins	0.971	11.81	34.9	4.00
1:1.2	90°C/6 mins	0.974	12.58	35.5	4.35
1:1.4	90°C/6 mins	0.964	13.22	37.0	4.71
1:1.6	90°C/6 mins	0.964	13.04	35.8	4.49
1:1.7	90°C/6 mins	0.962	12.99	37.4	4.68
1:1.8	90°C/6 mins	0.959	13.05	36.1	4.52

Table S3. Photovoltaic performance of the solar cells based on **PD-1:L8-BO** under different D/A ratios with the addition of 4,5-difluorobenzo[c][1,2,5]thiadiazole (SF-2).

D:A	additives	w%	TA	V_{oc} (V)	J_{sc} (mA cm ⁻²)	FF (%)	PCE (%)
1:1.2	SF-2	120%	90°C/6 mins	0.963	13.82	40.9	5.44
1:1.4	SF-2	120%	90°C/6 mins	0.945	13.43	43.6	5.52
1:1.6	SF-2	120%	90°C/6 mins	0.935	12.99	44.9	5.45
1:1.7	SF-2	120%	90°C/6 mins	0.953	12.34	44.4	5.24

Table S4. Photovoltaic performance of the solar cells based on **PD-2:L8-BO** with different D:A ratios under the illumination of AM 1.5G.

D:A	TA	V_{oc} (V)	J_{sc} (mA·cm ⁻²)	FF (%)	PCE (%)
1:0.8	100°C/5 min	0.928	22.80	64.6	13.62
1:1	100°C/5 min	0.920	24.67	63.8	14.42
1:1.2	100°C/5 min	0.916	24.55	63.7	14.29
1:1.4	100°C/5 min	0.915	24.52	61.5	13.77
1:1.6	100°C/5 min	0.905	24.86	54.1	12.13

Table S5. Photovoltaic performance of the solar cells based on **PD-2:L8-BO** (1:1, w/w) with different additives under the illumination of AM 1.5G.

additives	content	TA	V_{oc} (V)	J_{sc} (mA·cm ⁻²)	FF (%)	PCE (%)
DIO	0.35 v%	100°C/5 min	0.905	25.32	66.7	15.24
DIO	0.5 v%	100°C/5 min	0.893	23.70	61.9	13.08
1-CN	0.35 v%	100°C/5 min	0.909	25.16	66.7	15.21
1-CN	0.5 v%	100°C/5 min	0.903	25.30	67.0	15.29
TT-Cl	100 w%	100°C/5 min	0.918	24.20	69.9	15.50
TT-Cl	120 w%	100°C/5 min	0.923	24.44	67.9	15.29
TT-Cl	150 w%	100°C/5 min	0.931	22.82	68.3	14.48
SF-2	100 w%	100°C/5 min	0.908	24.75	69.9	15.68
SF-2	120 w%	100°C/5 min	0.905	24.90	70.0	15.74
SF-2	130 w%	100°C/5 min	0.910	25.60	71.5	16.34

Table S6. Photovoltaic performance of the solar cells based on **PD-2** with different acceptors under the illumination of AM 1.5G.

D:A	Acceptors	V_{oc} (V)	J_{sc} (mA·cm ⁻²)	FF (%)	PCE (%)
1:1	Y6	0.857	26.34	66.6	15.03
1:1	L8-BO-X	0.901	25.37	62.4	14.26
1:1	BTP-eC9	0.868	25.59	65.9	14.64

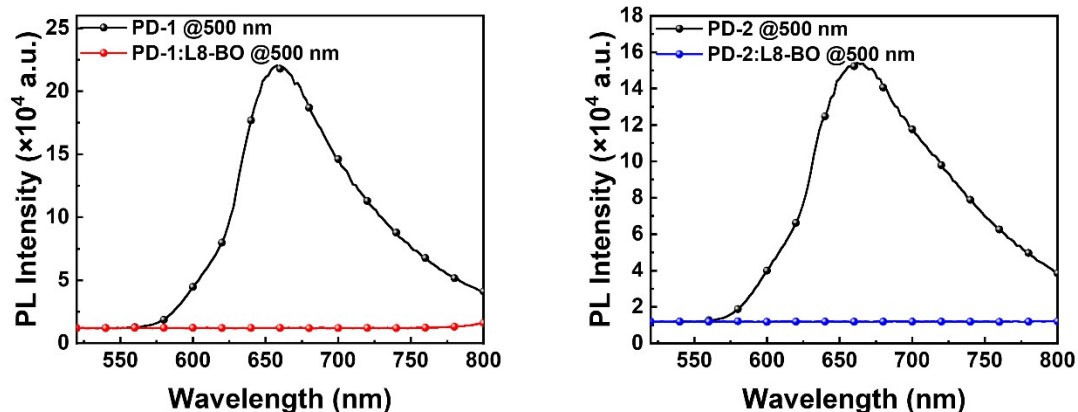


Figure S6. Photoluminescence spectra of PD-1, PD-2 neat films, PD-1:L8-BO and PD-2:L8-BO blend films. All films are excited by 500 nm wavelength.

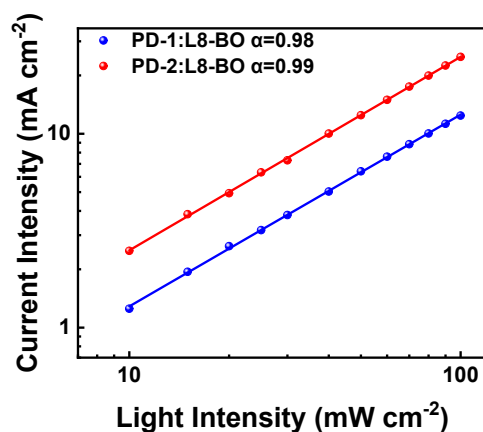


Figure S7. J_{sc} vs. light intensity of OSCs.

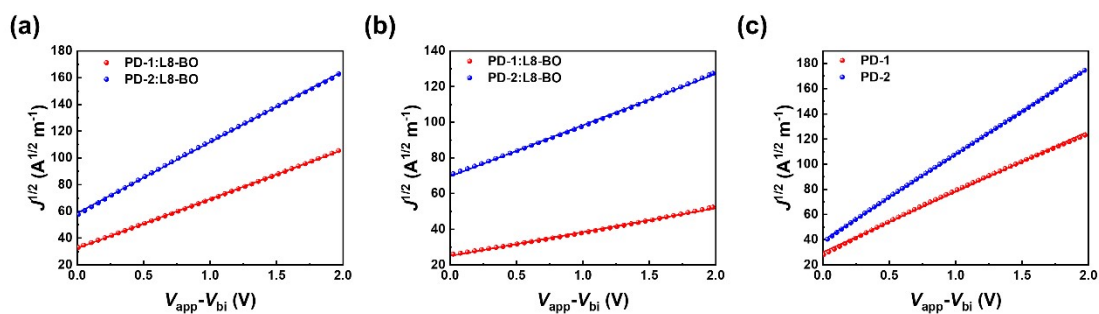


Figure S8. (a) Measurement of hole mobilities of PD-1:L8-BO and PD-2:L8-BO blend films; (b) Measurement of electron mobilities of PD-1:L8-BO and PD-2:L8-BO blend films. (c) Measurement of hole mobilities of PD-1 and PD-2 pristine films.

Table S7. Total energy loss values and different contributions in organic solar cells based on the SQ limit theory.

Device	E_g^a (eV)	V_{oc} (V)	$V_{oc,sq}^b$ (V)	$V_{oc,rad}^c$ (V)	ΔE_1 (eV)	ΔE_2 (eV)	ΔE_3^d (eV)	ΔE_3^e (eV)	E_{loss} (eV)
PD-1:L8- BO	1.449	0.945	1.182	0.99	0.267	0.080	0.157	0.174	0.504
PD-2:L8- BO	1.459	0.910	1.191	1.03	0.268	0.098	0.183	0.246	0.549

^a. E_g was determined by FTPS-EQE spectra of devices; ^b. $V_{oc,sq}$ is calculated according to the SQ limit; ^c. $V_{oc,rad}$ is the V_{oc} when there is only radiative recombination and is calculated from the EQE, FTPS-EQE and EL measurements; ^d. ΔE_3 was calculated by $q(V_{oc,rad}-V_{oc})$; ^e. ΔE_3 was obtained from the equation $q\Delta V_{nr} = -kT\ln EQE_{EL}$ by measuring the device EQE_{EL} .

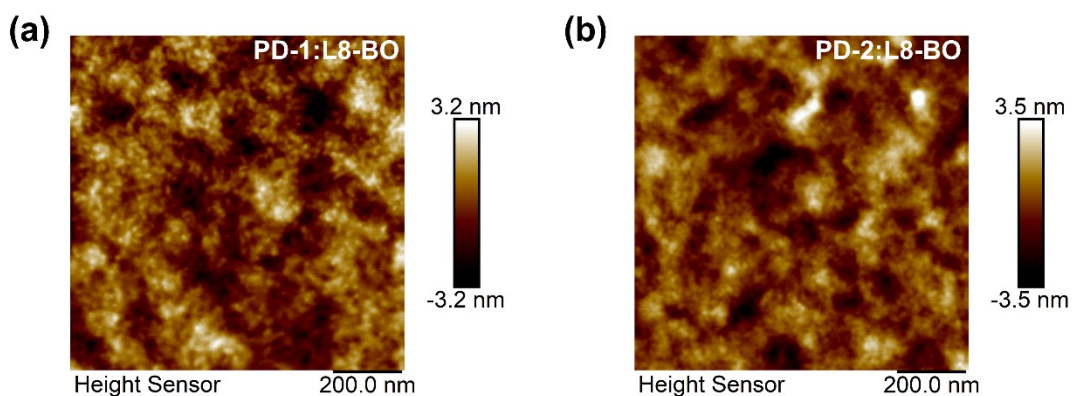


Figure S9. AFM height images of PD-1:L8-BO and PD-2:L8-BO blend films.

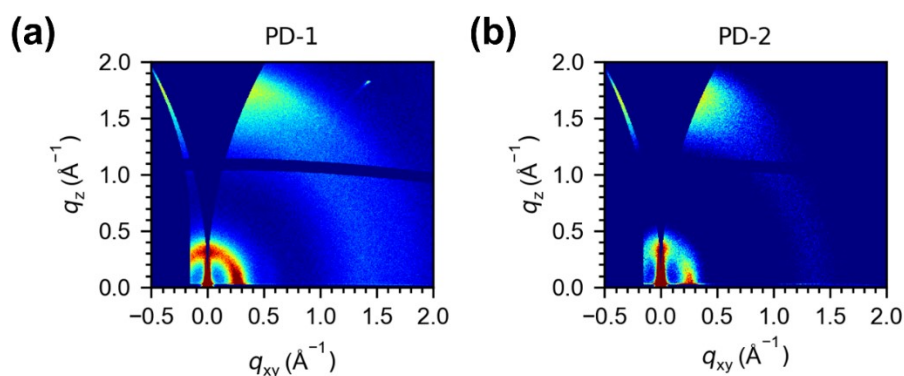


Figure S10. 2D GIWAXS patterns of the neat films of PD-1 and PD-2, respectively.

Table S8. GIWAXS measurement performance parameters of the related films

Compound	OOP				IP			
	(010)				(100)			
	q (\AA^{-1})	d - spacing (\AA)	FWHM (\AA^{-1})	CL (\AA)	q (\AA^{-1})	d - spacing (\AA)	FWHM (\AA^{-1})	CL (\AA)
PD-1	1.72	3.65	0.354	15.97	0.274	22.93	0.085	73.92
PD-2	1.65	3.81	0.434	13.03	0.261	24.07	0.346	18.16
PD-1:L8-BO	1.69	3.72	0.365	15.49	-	-	-	-
PD-2:L8-BO	1.67	3.76	0.671	8.43	0.287	21.89	0.052	120.8

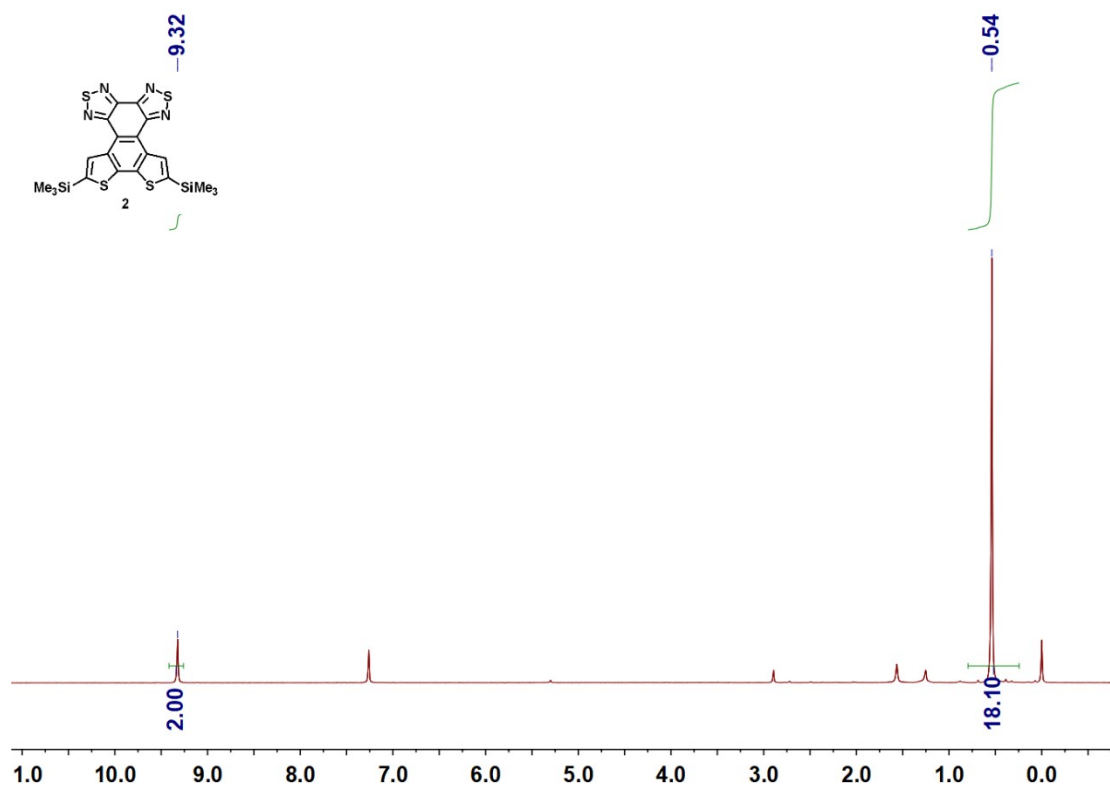


Figure S11. ^1H NMR spectrum of compound **2** at 300K in CDCl_3 .

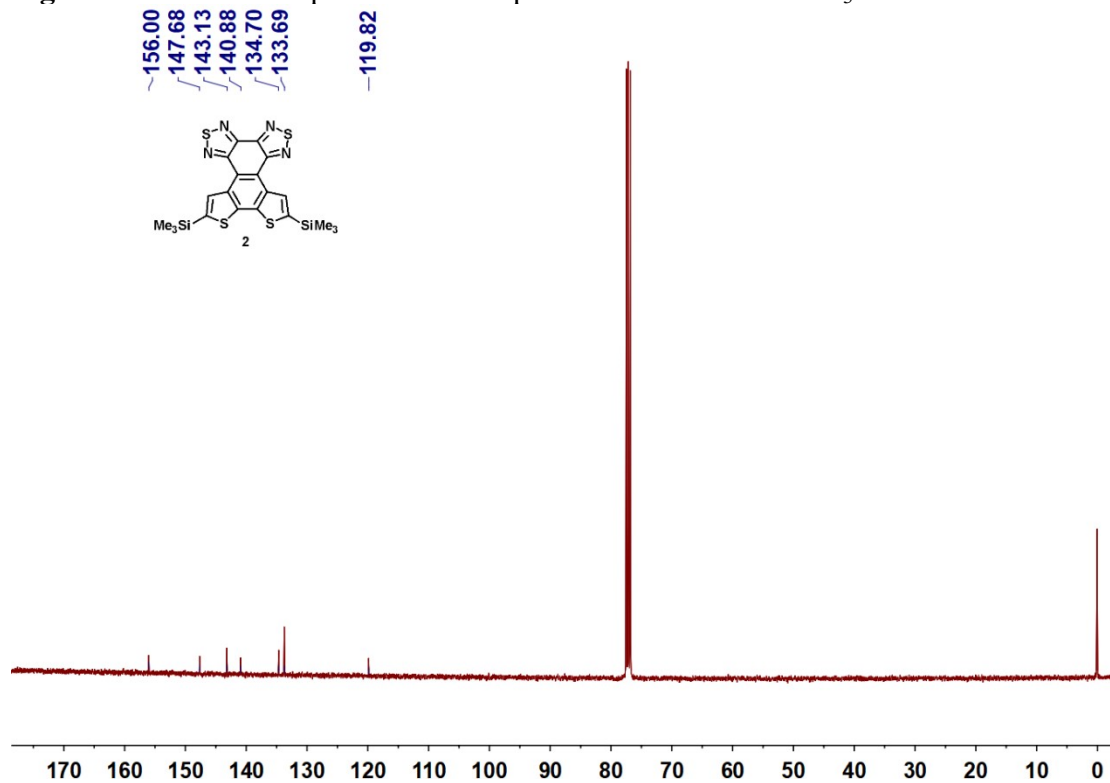


Figure S12. ^{13}C NMR spectrum of compound **2** at 300K in CDCl_3 .

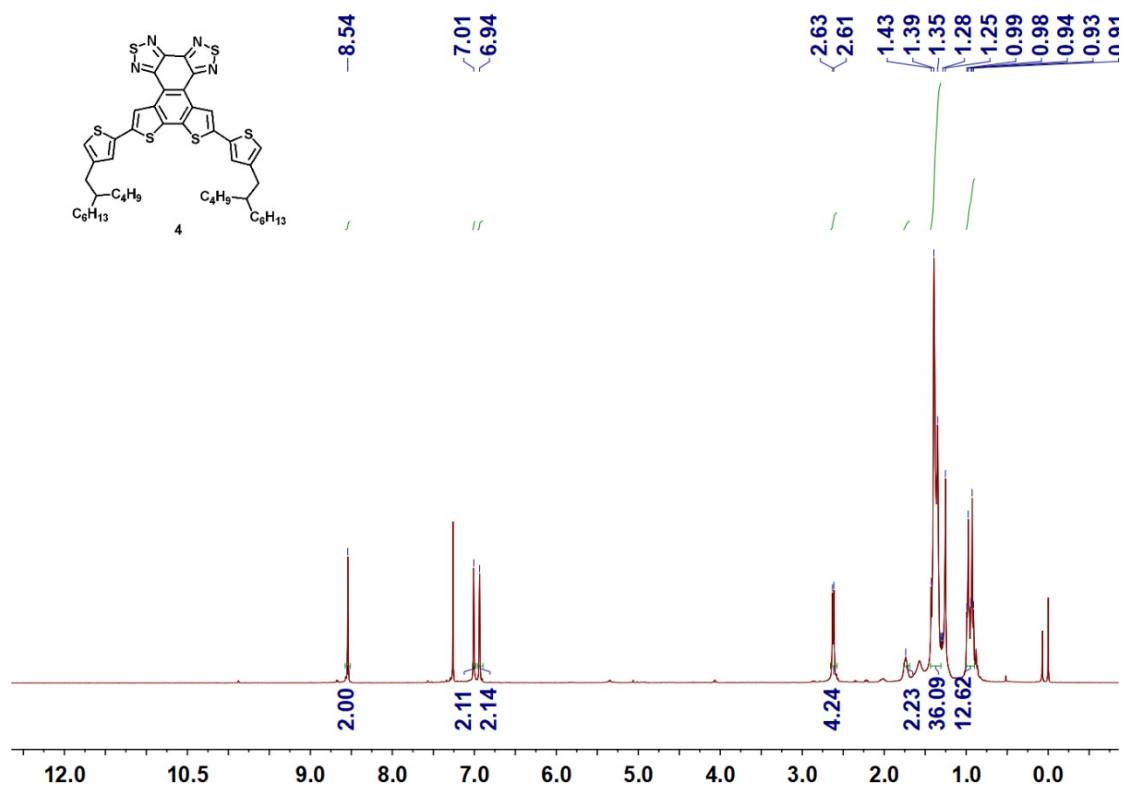


Figure S13. ¹H NMR spectrum of compound 4 at 300K in CDCl₃.

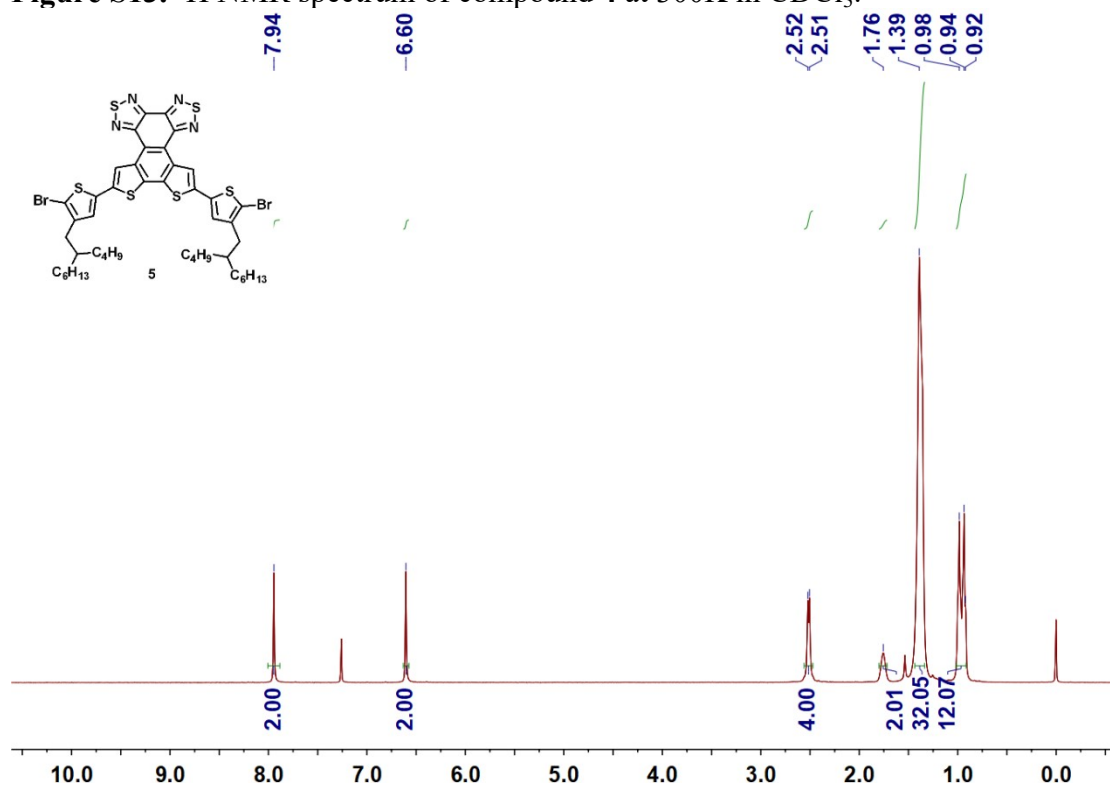


Figure S14. ¹H NMR spectrum of compound 5 at 300K in CDCl₃.

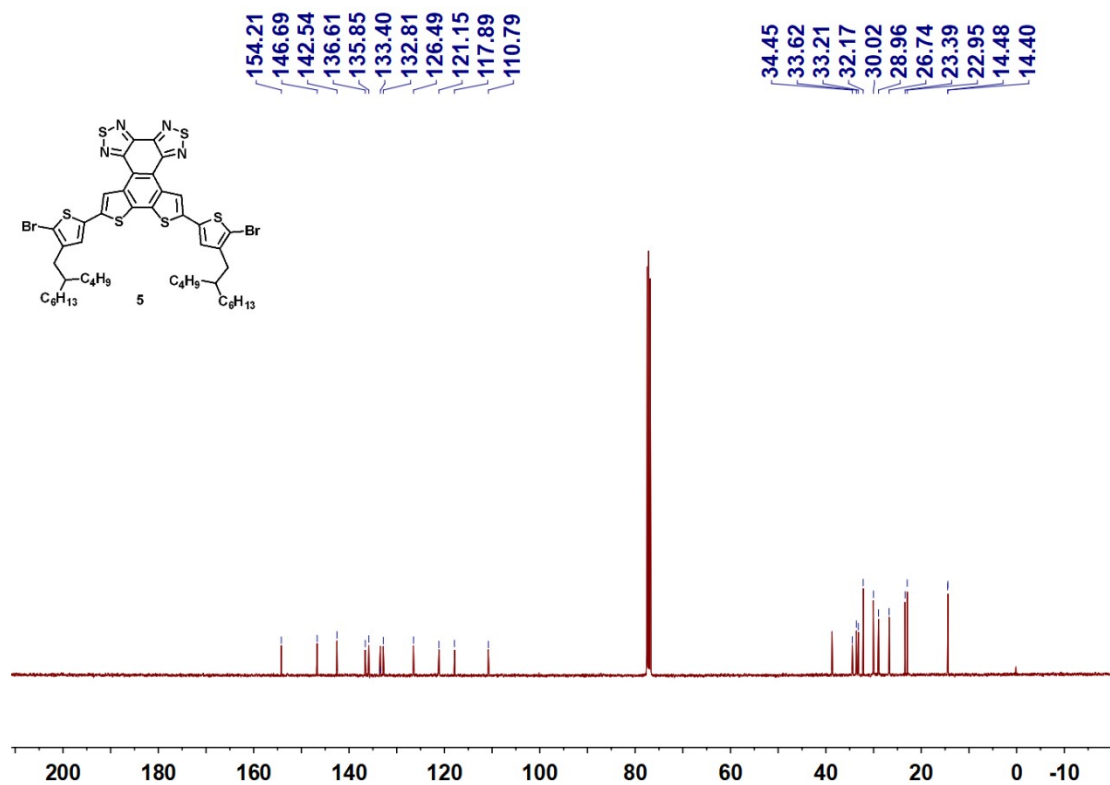


Figure S15. ¹³C NMR spectrum of compound 5 at 300K in CDCl₃.

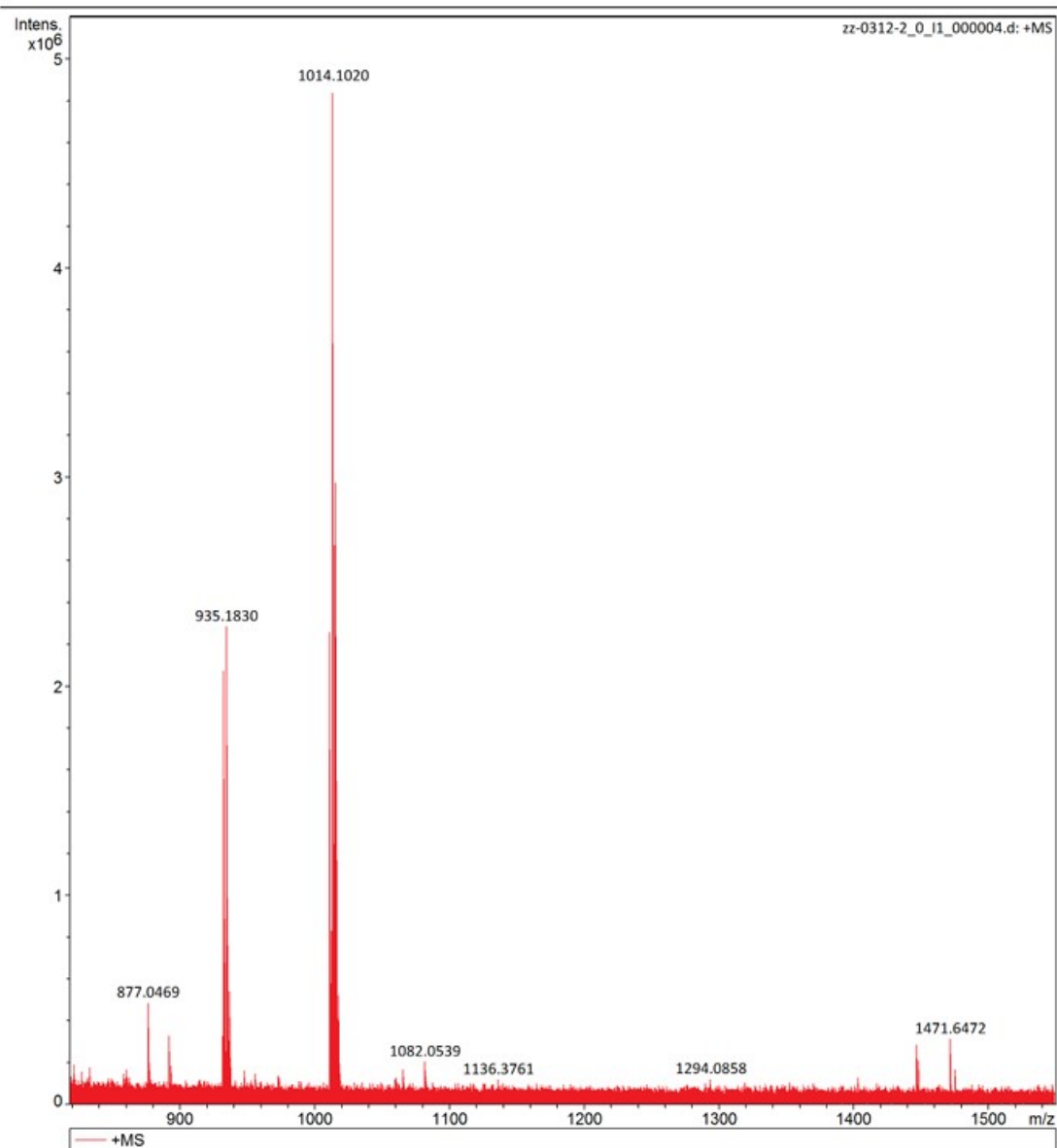


Figure S16. HRMS spectrum of compound **5**.

MW Averages

Mp: 49662 Mn: 19175 Mv: 47494 Mw: 53050
Mz: 96837 Mz+1: 142611 PD: 2.7666

Distribution Plots

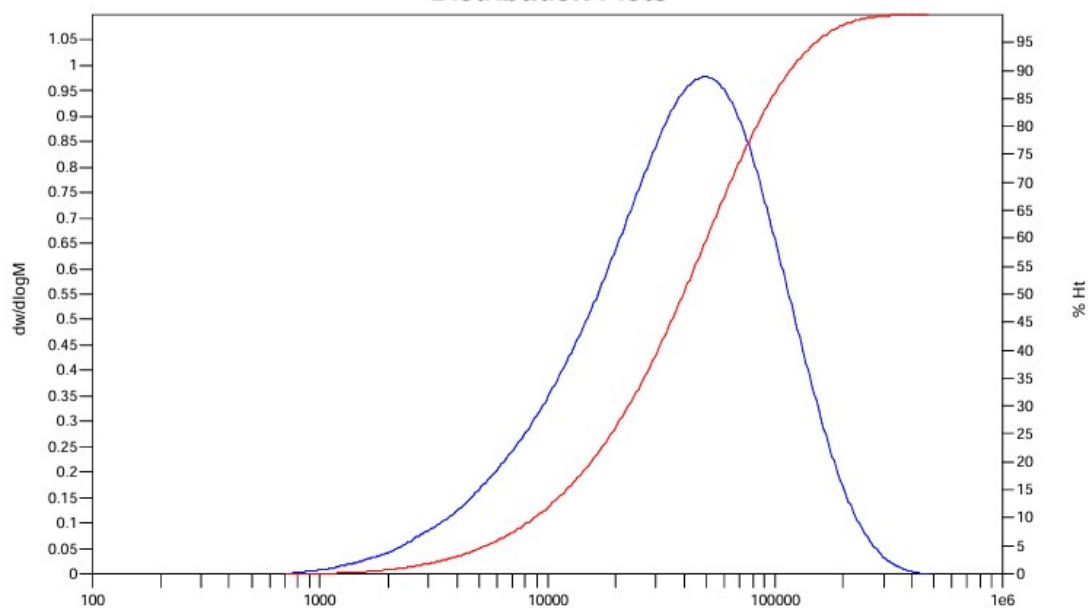


Figure S17. GPC curve of polymer PD-1.

MW Averages

Mp: 103249 Mn: 47768 Mv: 95607 Mw: 104190
Mz: 164674 Mz+1: 215412 PD: 2.1812

Distribution Plots

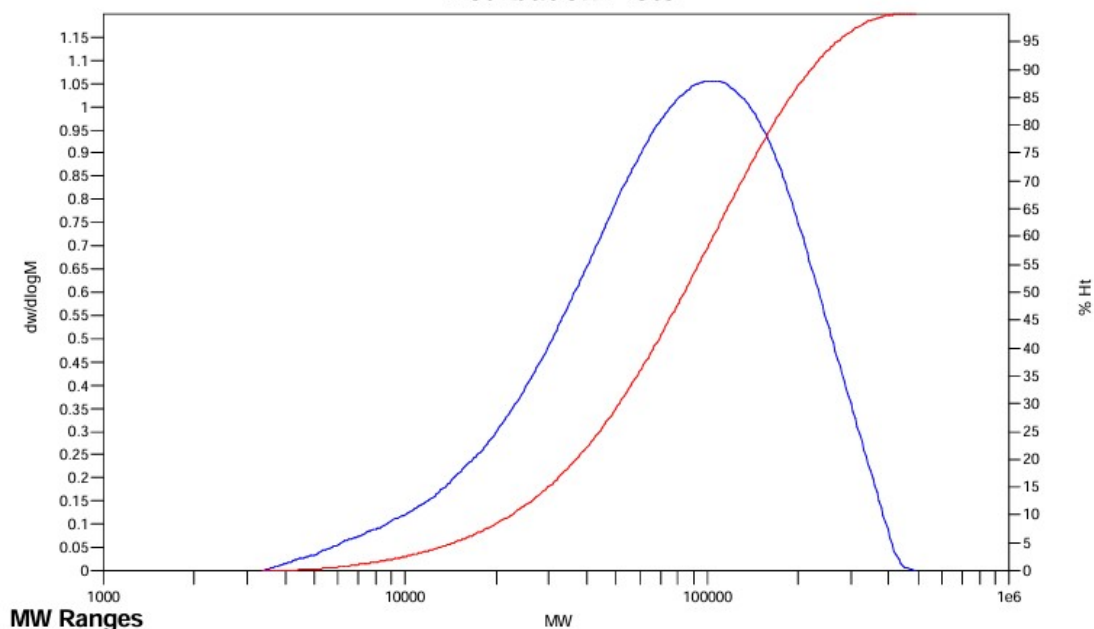


Figure S18. GPC curve of polymer PD-2.

References

1. A. S. Chechulina, L. S. Konstantinova, N. V. Obruchnikova, E. A. Knyazeva, B. Kan, T. Duan, Y. Chen, R. A. Aysin and O. A. Rakitin, *Chem. Heterocycl. Compd.*, 2024, **60**, 403-408.
2. J. Chen, D. Li, M. Su, Y. Xiao, H. Chen, M. Lin, X. Qiao, L. Dang, X. C. Huang, F. He and Q. Wu, *Angew. Chem., Int. Ed.*, 2023, **62**, e202215930.